

DEFORMATION AND DISRUPTION OF SILVER WIRES

S. Arai

INTRODUCTION A series of swellings is often observed on the surface of a wire subjected to a large over-current. The formation of these swellings, the unduloids, was first studied by Kleen (1), who explained it by the surface tension acting on the molten surface of the wire. Afterwards, Baxter (2) attributed the stepwise voltage build-up across the terminals of a fuse to the formation of series of arcs at the nodes of the unduloid. However, it should be noted that quite different deformations from unduloids are observed on the flash X-ray photographs taken for silver wires subjected to a very large current.

This paper is concerned with such deformations. The first chapter describes the flash X-ray tube and the associated measuring devices. The second chapter gives some typical X-ray photographs and the associated oscillograms of voltage and current wave-forms. The third chapter discusses the pinch effect considered to be responsible for the deformations.

FLASH X-RAY PHOTOGRAPHY The flash X-ray tube used for this study is illustrated in Fig. 1, where A is the anode of a sharp-pointed tungsten rod, C is the cathode of a stainless-steel disc with a hole in its centre, and T the triggering electrode of the same material and form as the cathode. These electrodes are contained in the glass vessel V, where the pressure is maintained below 10^{-4} mmHg by a vacuum pump. W is the X-ray window of vinyl resin film. The applied voltage on the anode is about 100 kv, which is supplied from the high voltage source consisting of capacitors, solid rectifiers and auxiliary equipments. When the triggering voltage of about 10 kv is impressed between the triggering electrode and the earthed cathode, it triggers the spark-over between the cathode and the anode, which radiates a strong X-ray beam of so short a duration (less than $1 \mu s$) through the window. The beam produced at the point of the anode, provides clear-cut silhouett of the wire on the X-ray film.

Fig. 2 illustrates the arrangement for the experimental study composed of LC-circuit, flasf X-ray device, delay system, and dual-beam oscilloscope. The condenser capacity of the LC-circuit was $1 \times 10^4 \sim 5.4 \times 10^5 \mu F$, the frequency of the LC-circuit was $3 \sim 200$ Hz.

The silver wires studied were 0.1, 0.2, 0.3, 0.4 and 0.5 mm in diameter and 5 cm in length. In order to avoid the unfavourable

Mr. Arai is with the Department of Electrical Engineering,
Tokyo Electrical Engineering College.

earlier disruptions at the ends of the wire due to lowering of the melting point by soldering, both ends of each wire were clamped by thin copper tubes and these tubes were soldered to the terminals. The wires were stretched in air or embedded in sand.

EXPERIMENTAL RESULTS The deformations of the wire from their starts to the disruptions are illustrated in Fig. 3. The voltage wave corresponding to the bright portion of the current wave is correlated with several sets of X-ray photographs. These photographs are of different wires taken at the indicated instants. Photograph (a) shows no deformation. In (b) slight deformation is observed, and in (c) and (d) the deformations are appreciable. Further, in (e) the disruptions of the molten wire are observed.

The fact that the point O on the voltage wave corresponds to the instant of completion of the liquefaction is ascertained by the measurement of the temperature near the melting point with a photomultiplier. Synchronized record of the voltage across the wire and the photomultiplier output is shown in Fig. 4. Since the thermal radiation during melting period must be constant, the duration of melting coincides with the time interval from t_1 to t_2 . Thus, the deformations occur in the liquid state of the wire.

Fig. 5 shows the deformations for linearly rising currents such as to give the same current density to the wires. Photograph (a), series of round swells are observed. In (c), however, squarish shapes of swells and necks are observed. It is interesting that the wedge-like fine deformations on the surface of the wire first appear always, on the concave side of the bent wire. It was also observed that the fine deformations of wires appeared earlier for thick wires than for fine wires.

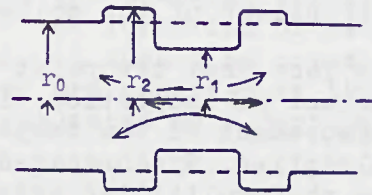
The deformations of 0.5 mm silver wire subjected to a large currents of about 50 Hz are shown in Fig. 6. In (a) melting time was 5 ms, cut-off current was 960 A. Sloping-shouldered swells and necks are observed. In (b) and (c), melting times were 2 and 1 ms and cut-off currents were 2 kA and 2.4 kA respectively. Squarish fine deformations are observed. In general, for larger currents swells and necks are more squarish.

The fine deformations of the wires embedded in sand are shown in Fig. 7. The deformations are always located near the summits of the waved wire due to the thermal expansion. Furthermore, they are observed only on that side of the wire which is pressed to the sand. It is considered that these observations support Vermij's observations (3) that the time from the instant of the completion of liquefaction to the disruption of the wire embedded in sand is shorter than that of the wire stretched in air.

INTERPRETATION DUE TO PINCH EFFECT It may be supposed that surface tension, electromagnetic force and thermal stress give rise to the surface wave on the cylindrical liquid. This section suggests that the wires being affected by the electromagnetic pinch deform into series of swells and necks in accordance with the surface wave. It is well known that a cylindrical conductor carrying a current is subjected to pinch pressure, the distribution of which is given by the following:

$$P = \frac{1}{4} \mu_0 i^2 r_0^2 \left[1 - \left(\frac{r}{r_0} \right)^2 \right] \quad (N/m^2) \quad \dots\dots(1)$$

where μ_0 is the magnetic permeability of vacuum, i is the current density, r_0 is the wire radius and r is the lateral distance from axis. The maximum pressure occurs at the axis and is proportion to the square of the current density. Accordingly the very small irregularities due to the surface wave give rise to a longitudinal force difference acting in the direction from the smaller to the larger cross-section. This longitudinal difference of force gives rise to a flow in the liquid cylinder, making the neck smaller and smaller and the swell larger and larger. A model for the deformation is shown in Fig. 8, where r_1 is the radius of the neck and r_2 the radius of the swell. The flow from the neck to the neighbouring swells is illustrated in Fig. 8. Since the flowing liquid is incompressible, the following equations are obtained (Appendix)



$$t = T_0 \left[1.85 - F\left(\frac{1}{2}, \theta\right) \right] \quad \dots\dots(2)$$

$$\theta = \arcsin k \quad \dots\dots(3)$$

$$T_0 = \frac{4}{\epsilon \alpha} \left(\frac{\sigma}{\mu_0} \right)^{\frac{1}{2}} \frac{\pi r_0^2}{I} \quad \dots\dots(4)$$

Fig. 8. A model for the deformation

, where t is the time measured from the initiation of deformation,

$F\left(\frac{1}{2}, \theta\right)$ the elliptic integral of

the first kind, α the flow coefficient, ϵ the ratio of the length of the neck to r_0 , σ the density of the wire, I the current flowing through the wire, and k the ratio of r_1 to r_0 . The radius of neck reduces with time, until at last the wire disintegrates. The time from the start of deformation to the disintegration T_d is given as follows:

$$T_d = \frac{7.4}{\epsilon \alpha} \left(\frac{\sigma}{\mu_0} \right)^{\frac{1}{2}} \frac{1}{i_0} \quad \dots\dots(5)$$

where i_0 is the apparent current density which is the current divided by the original cross section of the wire before the current flow.

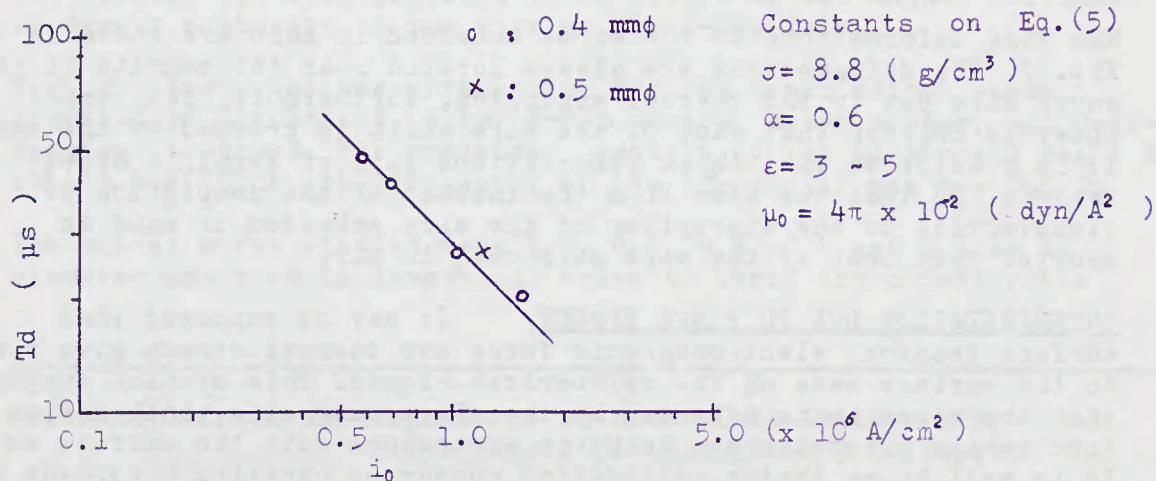


Fig.9. Relations between the apparent current density and the time from the start of deformations to the disruptions by pinch action.

The relations between T_d and the apparent current density i_0 calculated from Eq. (5) for silver wires with the measured values of ϵ are shown in Fig.9. And the relations of T_d versus i_0 are plotted on the figure. They are given by the time from the instant the photograph was taken to the arcing, ϵ and r/r_0 of smallest neck at the instant the photograph taken and Eq.(2). A good agreement between the measured results and the analytical results is recognized.

Since the action of pinch effect to the deformations depends upon the current and the diameter of wire, the deformations of the wires of larger diameter due to the very large current are predominantly affected by pinch effect. Accordingly the pattern of the deformation of the wires of large diameters is sharply squarish.

In the case of the wire of smaller diameter or moderately large current flowing through the wire, it may be considered that both the pinch effect and the surface tension would take parts in the deformations and that the pattern of the deformations would be modified as shown in Fig. (5),(6).

SUMMARY For silver wires subjected to very large over-currents, we observed the deformations of the wires just before the initiation of the arcing with a flash X-ray apparatus and a dual beam oscillograph.

It was recognized that the deformations took place after the complete liquefaction of the silver wires. The sharply squarish shapes of necks and swells were observed under conditions of very high current density and the wire of large diameter. The rounded necks and swells were observed on the wire of small diameter or moderate currents.

It is considered that in the case of larger currents flowing through wires of larger diameters, the deformations are caused by pinch effect, and that for moderate current densities or in wires of smaller diameters, the deformations are due both to pinch effect and surface tension.

Since the wires embedded in sand are subjected to the pressed contact with around sand, the fine deformations of the wires occur relatively early after the completion of liquefaction and they are located near the summit of the waved wire.

It is recognized that the stepwise voltage rise corresponds to successive arc initiations at some of the necks.

AKNOWLEDGEMENTS The author is very grateful to Professor A. Hirose for his valuable advice and very detailed discussion. He also wishes to thank the Matsunaga Science Foundation and the Saneyoshi Shogaku Kai for the financial help.

REFERENCES (1) Kleen, W. Ann. Physik 5. 11(1931)579.
 (2) Baxter, H.W. Electric Fuses . Arnold London(1950).
 (3) Vermij, L. Electrical Behaviour of Fuse Elements(Thesis).

APPENDIX In Fig. 8, flow is divided at the center of the neck.

Since the liquid is incompressible, the following relation is obtained

$$r_1 = k r_0 \quad \dots\dots(6)$$

$$r_2 = (2-k^2)^{\frac{1}{2}} r_0 \quad \dots\dots(7)$$

The critical radius r_3 , for which the pressure in the neck is equal to the pressure in the swell is given

$$r_3 = k (1 - \frac{1}{2}k^2)^{\frac{1}{2}} r_0 \quad \dots\dots(8)$$

Within the circle of the radius r_3 , flow occurs from the neck to the swell. Let \bar{P}_1 and \bar{P}_2 be respectively the mean pressure in the neck and in the swell, then the exit velocity is shown as follows:

$$\bar{v} = [\frac{2}{\sigma} (\bar{P}_1 - \bar{P}_2)]^{\frac{1}{2}} \quad \dots\dots(9)$$

The volume of fluid that leaves the neck during the infinitesimal time interval dt is

$$dQ = \alpha \pi r_3^2 \bar{v} dt = \frac{1}{4} \alpha (\frac{2\mu_0}{\sigma})^{\frac{1}{2}} I r_0 k [(1-k^2)(2-k^2)]^{\frac{1}{2}} dt \quad \dots\dots(10)$$

on the other hand, the outflowing volume is

$$dQ' = 2\pi r_1 dr_1 \frac{r_0}{2\varepsilon} = \frac{\pi}{\varepsilon} r_0^3 k dk \quad \dots\dots(11)$$

Since dQ must be equal to dQ' , we obtain a function of t and k as follows:

$$dt = \frac{8}{\varepsilon \alpha} (\frac{\sigma}{2\mu_0})^{\frac{1}{2}} \frac{\pi r_0^2}{I} \frac{dk}{[(1-k^2)(2-k^2)]^{0.5}} \quad \dots\dots(12)$$

The above differential equation is integrated between $t=0$ and t with respect to t for the left-hand side and between $k=1$ and k with respect to k for the right-hand side, Eq.(2) is obtained.

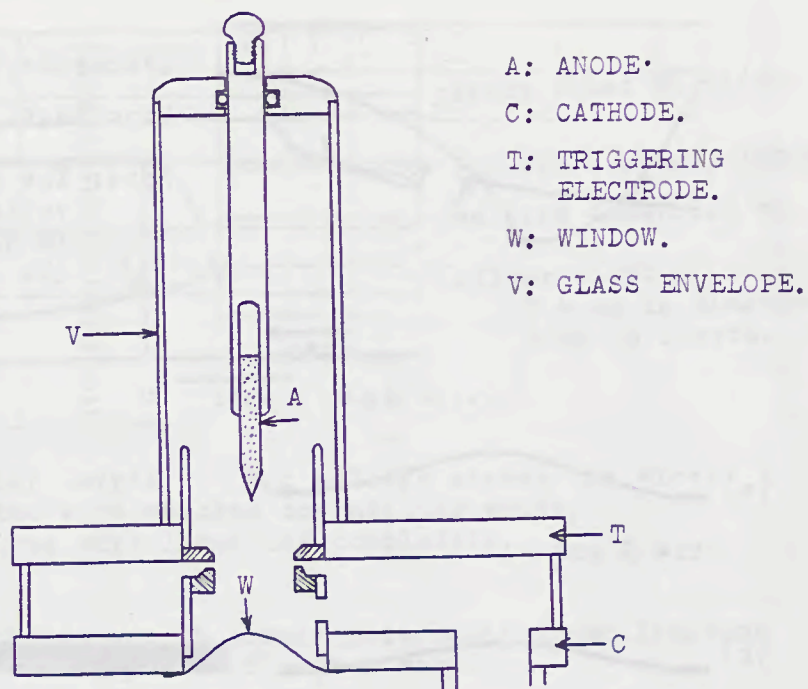
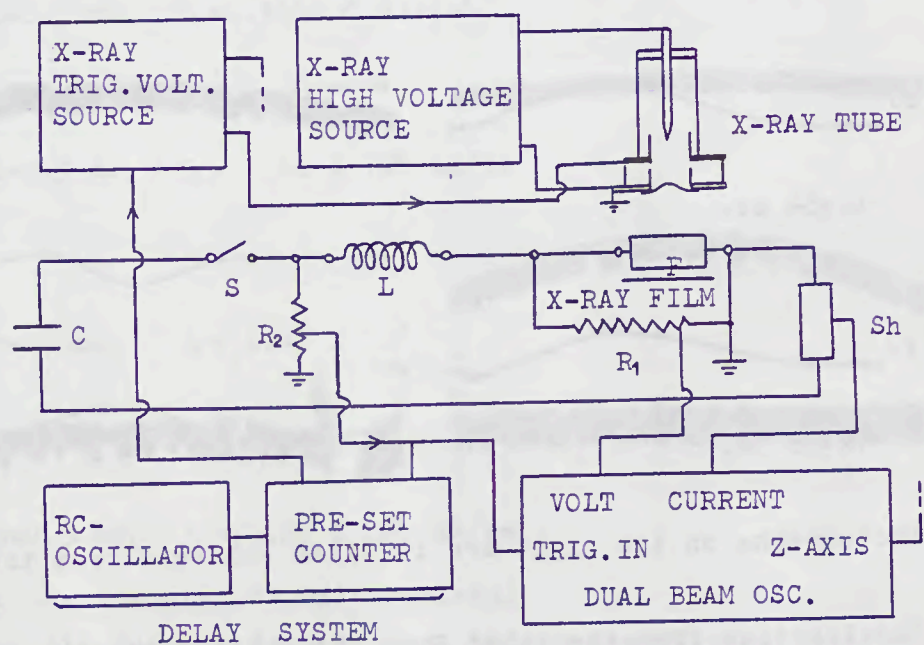
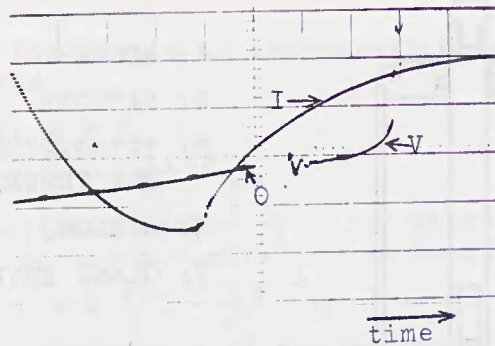


Fig. 1 Flash X-ray Tube.



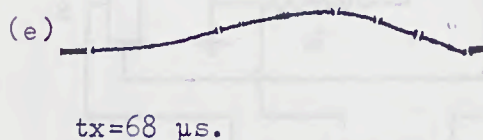
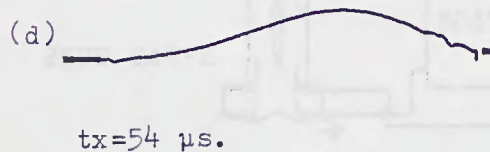
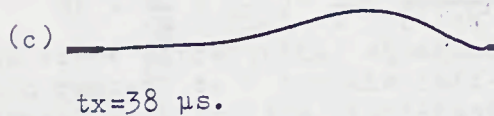
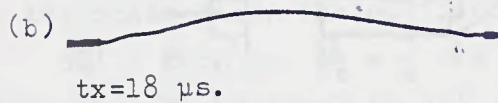
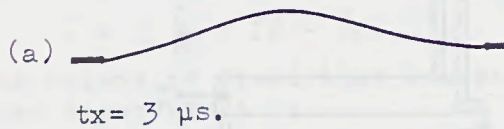
C: CONDENSER, L: REACTOR, S: SWITCH, F: SAMPLE,
R₁: VOLTAGE DIVIDER, R₂: VOLTAGE DIVIDER,
Sh: CO-AXIAL CURRENT SHUNT.

Fig. 2 Block diagram of experimental apparatus.



I: current, sweep time 0.5ms/div.
V: voltage, sweep time 20 μ s/div.

Note: The overall time of the voltage wave corresponds to the bright portion of the current wave.



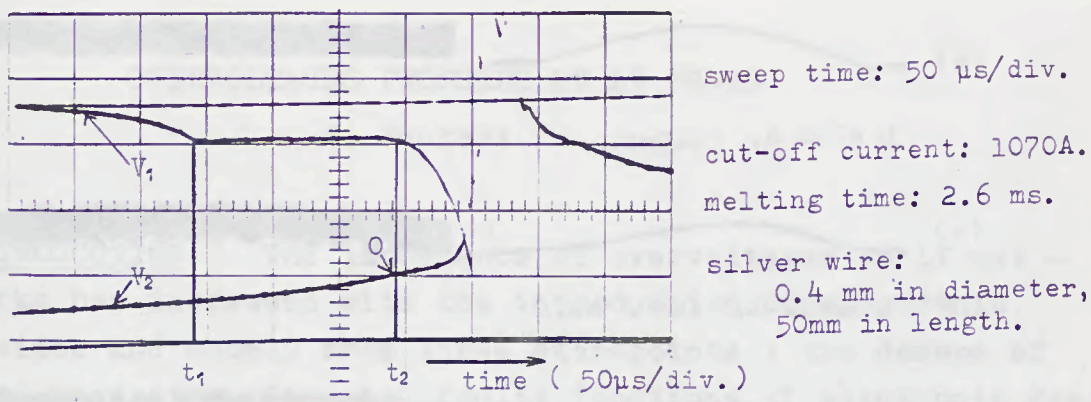
Photographs on the right are 10 times enlarged from the left.

tx: the time from the point 0 on the voltage wave on the oscillograph to the instant the photograph was taken.

Silver wire: 50 mm in length, 0.5 mm in diameter.

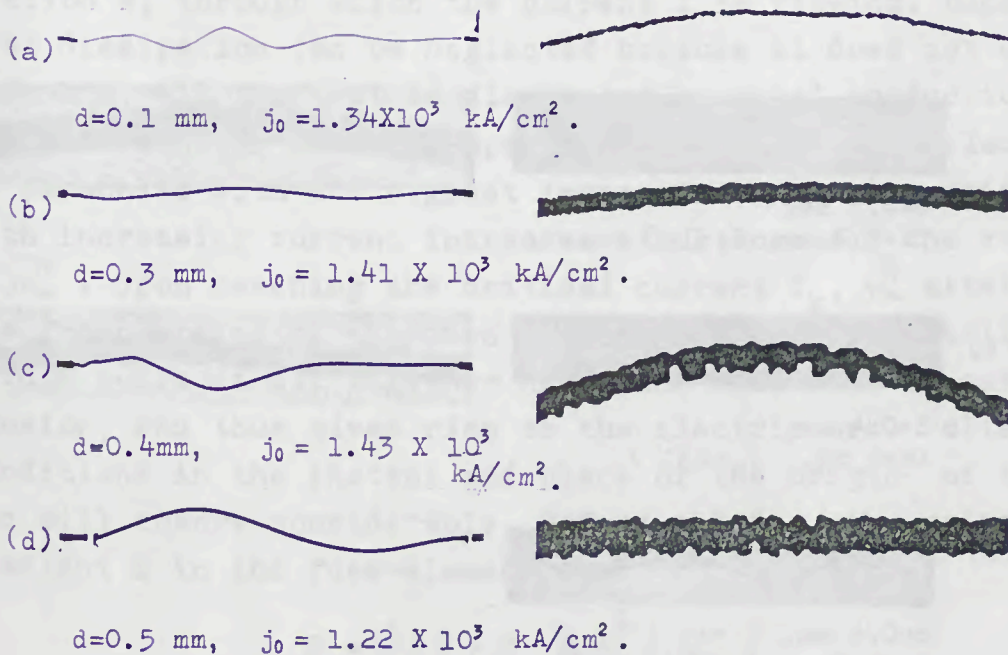
Melting time: 2 ms, cut-off current: 815 A.

Fig. 3 X-ray photographs of deformations and disruptions of silver wires stretched in air and V and I oscillogram.



V_1 : photomultiplier output, V_2 : voltage across the wire.
 t_1 : the instant, the wire reached the melting point,
 t_2 : the instant, the wire liquefied completely.

Fig. 4 Typical voltage and photomultiplier-output oscillograms near the melting point of silver wire.

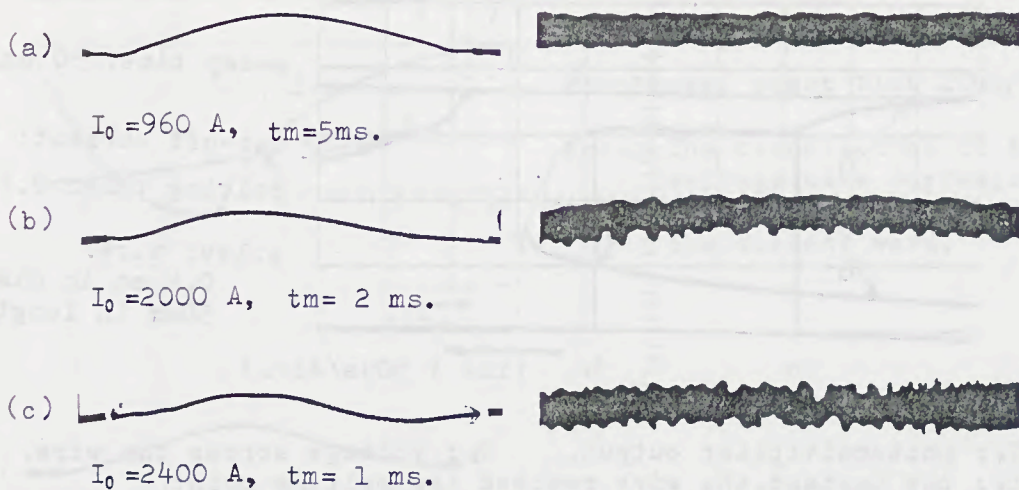


d : the diameter of silver wires.

j_0 : the current density just before the arc-initiation.

Photographs on the right are 10 times enlarged from the left.

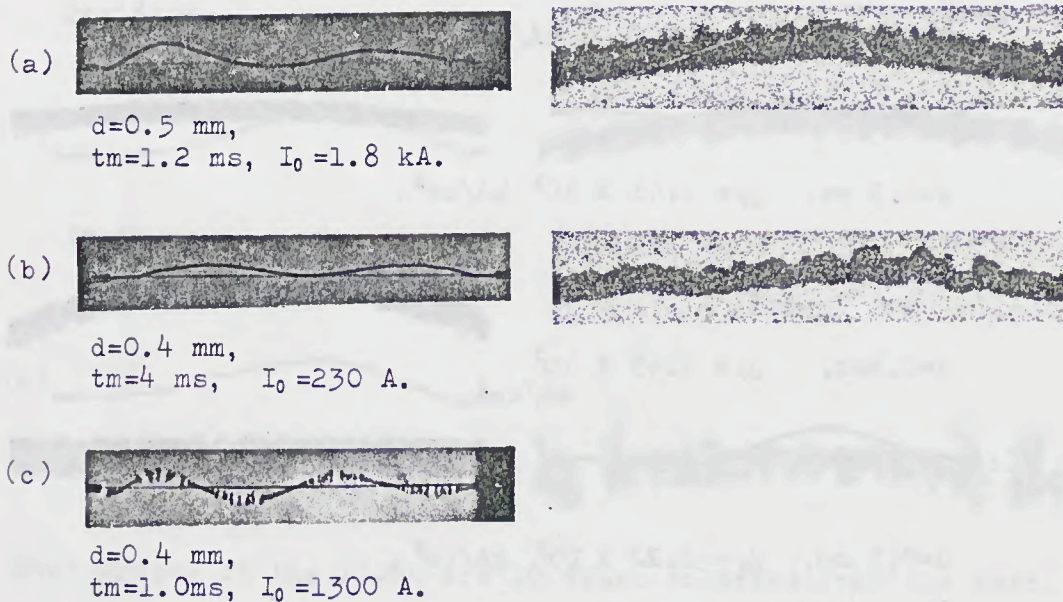
Fig. 5 X-ray photographs of deformations of the various silver wires for constant current density.



Photographs on the right are 10 times enlarged from the left.
Silver wire: 0.5 mm in diameter, 50 mm in length.

I_0 : cut-off current. t_m : melting time.

Fig.6 X-ray photographs of deformations of silver wires for various values of current.



Photographs on the right are 10 times enlarged from the left.

d : the diameter of wires, the length of wires is 50mm.

t_m : melting time, I_0 : cut-off current.

The mean diameter of grain of sand is 0.42 - 0.32 mm.

Fig.7 X-ray photographs of deformations and disruptions of silver wires embedded in sand.